Characterization of MDF Reinforced with Al_2O_3 Nano Particles Considering Physical, Mechanical and Quasi-static Properties

Sadaf Karkoodi[1]
[1] Master of Science in Applied Mechanics, Department of Mechanical Engineering, Tarbiat Modares University, Tehran, Iran, Email: s.karkoodi@modares.ac.ir

Gholamhossein Liaghat[2,3*]
[2*] Professor, Department of Mechanical Engineering, Tarbiat Modares University, Tehran, Iran, Tel: +98 21 8288 3387, Email: ghlia530@modares.ac.ir
[3*] Professor, Department of Mechanical Engineering, Kingston University, London, England, Tel: +44 20 8417 4813, Email: g.liaghat@kingston.ac.uk

Hamid Zarea Hosseinabadi[4]
[4] Assistant Professor, Wood-based Products, Department of Wood and Paper Sciences and Technology, Natural Resources Faculty, College of Agriculture and Natural Resources, University of Tehran, Karaj, Iran, Email: hzareah@ut.ac.ir

Hamed Ahmadi[5]
[5] Assistant Professor, Department of Mechanical Engineering, Tarbiat Modares University, Tehran, Iran,
Email: h_ahmadi@modares.ac.ir

Abstract

The paper investigates the addition of Nano-Al_2O_3 powder (alumina, Average Particle Size: 20nm) on the characteristics of the Medium Density Fibreboards (MDF) made by the forest fibers. Some important physical, mechanical and quasi-static properties of the panels were measured according to the standard test methods and apparatus. Different percentages of alumina powder (0, 1, 2, and 3 weight percentage (wt.) based on the solid content of resin) were used and panels were made in three thicknesses (5, 10 and 14 mm). The experiments showed that the resultant properties of the new composites were improved. The greatest increase in Modulus of Elasticity (MOE) was achieved when 1% wt. alumina was added to the samples. Addition of alumina up to 1% wt. in 5 and 10 mm panels amplified energy absorption by 17% and 24%, respectively. The greatest increase in peak load and energy absorption was observed in samples with 2 and 1 % wt. alumina, respectively. Finite element modelling was also used to validate the experimental results. The numerical modeling was in good agreement with the experimental results.

Keywords: Medium Density Fibreboard, Nano-Al_2O_3 Powder, Mechanical properties, Physical properties, Quasi-static properties, Finite Element Modeling

1. Introduction

Quite recently, natural fibre composites have substituted by synthetic fibers in order to achieve renewable and biodegradable products with fewer costs and weights desired for many applications such as aerospace, marine, automotive and energy industries. Wood as a green material plays a vital role in the environment because of its desirable properties (Glé et al. 2011, Liu et al. 2017). In this due, considerable attention has been paid to wood-based panels, composed of wood fibers bonded together by an interior thermoset resin (mostly urea or phenol-formaldehyde) under hot pressure named MDF. Many types of research have been conducted on MDFs to improve this precious composite(Yoshihara and Yoshinobu 2015, Mantanis et al. 2018, Ates et al. 2017, Mantanis et al. 2019).

For instance, In Ref. (Jonoobi et al. 2017) the effect of chemical treatment, physical and mechanical characteristics on the fiber properties of the MDF were presented. Investigation of mechanical properties of the MDF showed that MOR and IB of the treated samples were decreased compared to the control ones. In Ref. (Benmansour et al. 2014), the possibility of using a new material consists of natural cement, sand and palm fibers was explored. It was observed that for the fiber loading lower than 15 %, the composite could be used for wall structures in buildings. Mechanical, thermal and insulating properties of ultra-light thick particleboard made from bagasse and wood planer shaving were investigated in Ref. (Hazrati-Behnagh et al. 2016). The result showed that the boards from bagasse and melamine-urea–formaldehyde resin had the best mechanical properties. Physical and mechanical properties of MDF panels made from kenaf and urea-formaldehyde were evaluated in Ref. (Aisyah et al. 2013). It is realized that the panels made from longer fibre had higher TS, MOR and MOE. In similar research on mechanical and physical properties of MDF composite materials, using recycled rubber, coconut coir and polyurethane as resin, experimental results show that the usage of MDF as filler enhances MOR, MOE, impact strength, hardness and density properties(Arabi et al. 2011).

There are several methods that can enhance the mechanical properties of MDF. Nanotechnology is a new approach to produce strong and lightweight materials with advanced features. The major drawback of this approach is the agglomeration of the reinforcing particles(Koli et al. 2014). There have been similar researches conducted on composites reinforced with nanoclay, showed an improvement in mechanical and thermal properties (Deka and Maji 2011a, Assaedi et al. 2016). In order to develop enhanced materials under quasi-static loading, understanding of the impact incidents and the damage mechanisms is strongly needed (Abrate 1991). It should be noted that impact issues can be classified in the following categories: low velocity impact (below 10 m/s) by a large mass, which is simulated using a falling weight or a swinging pendulum, and medium/high-velocity impact (10 to 50 m/s for medium velocity and 50 to 1000 m/s for high velocity) by a small mass, which is simulated with a gas gun or some other ballistic launchers (Abrate 2011, Cantwell and Morton 1991, Vaidya 2011). Some of the impact test researches on wood-based composites are as follows:

A new testing method measuring the specific fracture energy of wood-based panels in Mode I is done. Three types of wood-based panels, i.e. oriented strand board (OSB), particleboard (PB) and

MDF are investigated. IB results showed a large scattering of data, but the fracture energy test yielded statistically significant differences between the board types(Rathke et al. 2012).
CAI behavior of sandwich composite panels with intermediate pinewood and ash wood layers has been studied. It is observed that using wooden layers increased the residual CAI strength and decreased the depth of the impact damage (Balıkoğlu et al. 2018). A numerical model was developed to describe the fresh wood stem's response to a dynamic loading under quasi-static impact test (Olmedo et al. 2016). Four-point bend and Charpy testing were conducted to distinguish the mechanical behavior of maple and ash woods. The finite element model of the Charpy tests was simulated in LS-DYNA using the MAT_WOOD material model (Fortin-Smith et al. 2016). Damage results of balsa core sandwich composites, with thin carbon fiber skins, subjected to single and multiple sequential impacts were studied and the visual inspection and non-destructive tests showed that the damage was relatively localized (Jover et al. 2014).
Although several studies on the optimization of mechanical properties of panels are done, researches on enhancing natural composites are still lacking(Haseli et al. 2018). However, to the author's best knowledge very few publications can be found that discuss the effect of mixing Nano-ceramics with natural fibers in order to reinforce composites, while Nanotechnology is a novel methodology to achieve strong and lightweight materials with advanced features (Koli et al. 2014, Esmailpour et al. 2019).
This work explores reinforced MDFs with different percentages of alumina powder in three different thicknesses under low velocity punch test. The main aims were to study the changes in energy absorption, physical and mechanical properties of the MDF by considering the effect of its thickness and Nano Al_2O_3 weight percentage used in its resin content.

2. Material and methods

2.1. Material

In this research, the MDF is made from the feedstock, reinforced with Al_2O_3 nanoparticles. The fibers were dried at 101 ± 5 °C for at least 24 hours to the moisture content of 2% (dry-base) and kept in sealed plastic bags before processing(Hazrati-Behnagh et al. 2016). The feedstock was used as a matrix in this experiment. Industrial UF with specifications listed in Table 1, were provided from Tiran Chem. Company. NH_4Cl, which has 99.8% purity, the molecular weight of 53.49 gr and density of 1.52 g/cm^3, was used as a hardener in this experiment and the alumina (Al_2O_3, gamma, 99+%, and 20 nm) was used as a reinforcement.

Table 1. Specifications for UF resin

Resin Type	Specific gravity ($gr.cm^{-3}$)	Solid content (%)	Acidity	Viscosity (cP)	Gel Time (with hardener) (s)
UF	1.275	56	7.5-8	380	60

2.1.1 Field emission scanning electron microscopy (FESEM)

FESEM (model S-4160, Hitachi, Japan) with an accelerating voltage of 20 kV is applied to investigate the microstructures and distribution of nanoparticles. All samples were obtained by cutting the small piece of the prepared panels. All specimens were coated with a thin layer of gold to avoid charging.

2.1.2 Energy dispersive X-ray analysis (EDS)

The EDS was also performed on the interfacial microstructure. Although the EDS results are qualitative, an indication of the presence or absence of certain elements could be determined. By the EDS spectrum done on these specimen, It can be clearly seen that the peak of aluminum and oxygen elements are higher in the 3% Nano-alumina than the witness sample(Figure 1).

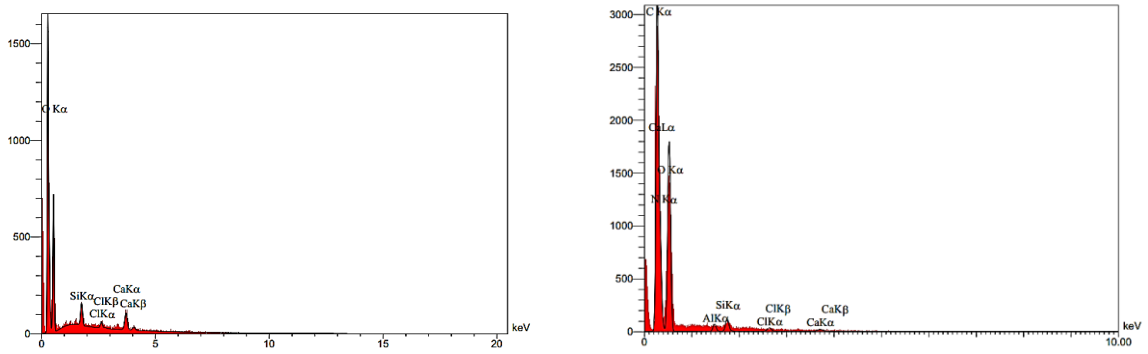

(a) **(b)**

Figure 1. EDS spectrum of a specimen. (a) with 0% alumina, (b) with 3% alumina

2.2 Sample Preparation

Formulations of the treatments used for the respective mixes are given in Table 2. The boards' thickness and the alumina percentage were considered as variables. Meanwhile, witness panels (nominal density 750 kg/m^3) were made with 12 wt. % glue (based on the oven-dry weight of fibers) without nanoparticles with the identical manufacturing parameters as other panels. Compound mixing was carried out in two stages, initially, the Nano was mixed with water by the homogenizer at 10,000 rpm for 5 minutes, and then the Nanofluid solution was added to a mechanical mixer with a rotation speed of 2000 rpm for 10 minutes with urea-formaldehyde adhesive. In the second phase, different percentage of Nano-Al_2O_3 powder (0, 1, 2, and 3 wt. % based on the solid content of resin) was added and boards were made in three thicknesses (5, 10 and 14 mm). The liquid UF resin was sprayed onto the wood fiber in a drum-type blender. Then the fibers were glued and poured into the wooden frame after being bonded. The resulting cake (Figure 2) was pressed at 170 ° C by the hydraulic hot press, BURKLE, Germany, and depending on the thickness of the boards (20 s per millimeter of boards' thickness) was sintered. The pressure for heating was 35 bar. After that, boards were cooled to room temperature. After cold stacking, all treated panels were kept in a conditioning chamber at 20 ± 3 °C and 65 ± 1 % RH for 2 weeks, in accordance with EN standard, until the panels reached the standard equilibrium moisture content.

Specimens are marked with the following instruction: S is the abbreviation for the word “Sample”. The first two numbers after S, refer to the thickness of the panels which are 05, 10, and 14 mm. The third number is the weight percentage of nanomaterials used in boards which varies from 0 to 3. For instance, S051 refers to a 5mm board with 1% wt. Nano Al_2O_3.

Table 2. Constant processing parameters for panel manufacturing

Processing parameter	Value
Ammonium chloride content (%UF)	2
Mat moisture content (% fiber)	12
Target density ($kg.m^{-3}$)	750
Frame Dimension (mm)	400×400
Nominal thickness (mm)	5,10,14
Press pressure ($kg.cm^{-2}$)	35
Press closing time ($mm.s^{-1}$)	4
Press temperature (°C)	170
Press time	20(s/mm)
Nano Al_2O_3 content(%UF)	1,2,3

Figure 2. The prepared mattress under the hot press

2.3. Characterization

2.3.1. Mechanical properties

The properties of IB, MOE, and MOR in dry conditions were investigated. The mechanical properties were conducted using a Universal Testing Machine (Instron 4486). Three iterations

were tested for each property under each configuration. The effects of thickness and Nano Al_2O_3 on the modulus of elasticity and modulus of rupture for boards are shown in Figure 3.

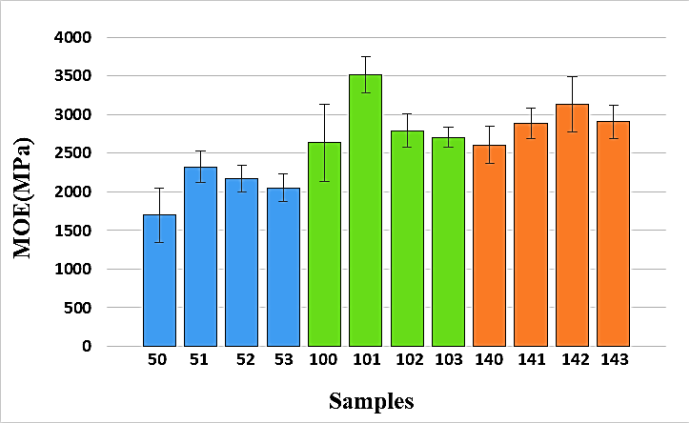

Figure 3a. Effects of thickness and Nano Al_2O_3 on the modulus of elasticity

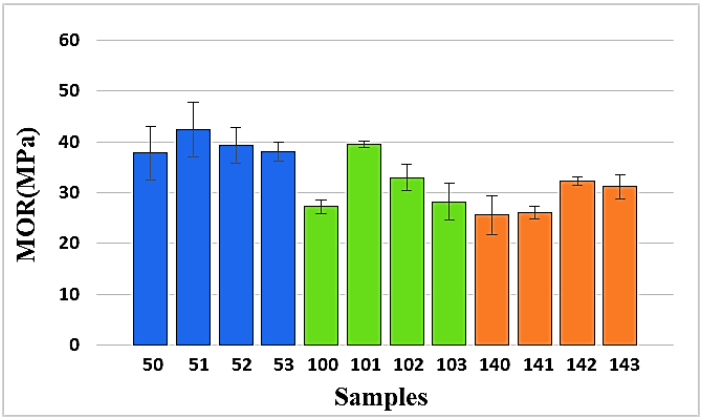

Figure 3b. Effects of thickness and Nano Al_2O_3 on the modulus of rupture

2.3.2. Physical properties

Physical properties (TS and WA), after 24-h cold water soaking was measured in accordance with EN standard methods (BS-EN-310 1993, BS-EN-317 1993, BS-EN-319 1993). Before testing, samples were weighed and dimensions were measured due to the EN standards (BS-EN-322 1993, BS-EN-323 1993). Three replications of each sample type were tested. The effects of thickness and Nanomaterial on the internal bonding of the boards are shown in Figure 4.

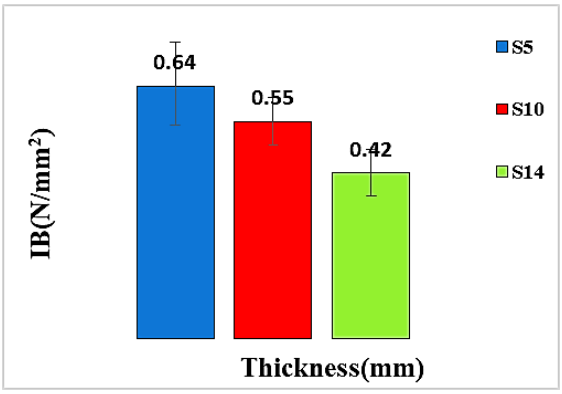

Figure 4a. Effects of thickness on the internal bonding

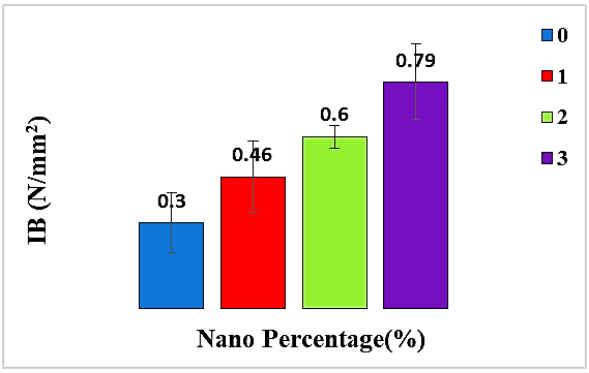

Figure 4b. Effects of adding Nanomaterial on the internal bonding

The effects of thickness and Nanomaterial on the water absorption of the boards are shown in Figure 5.

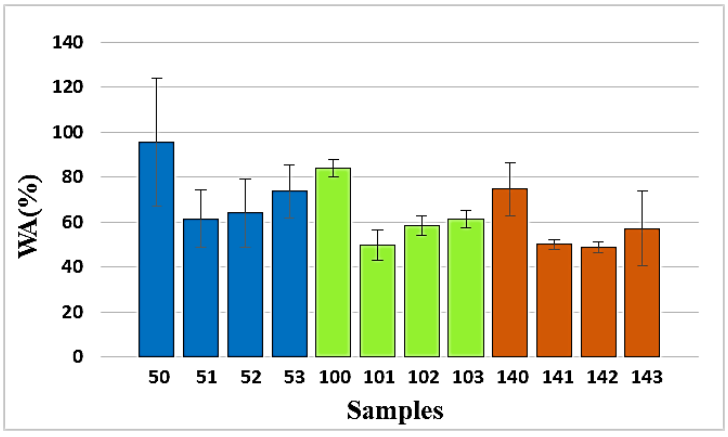

Figure 5. Effects of thickness and Nanomaterial on the water absorption

The effects of thickness and Nanomaterial on thickness swelling of the boards are shown in Figure 6.

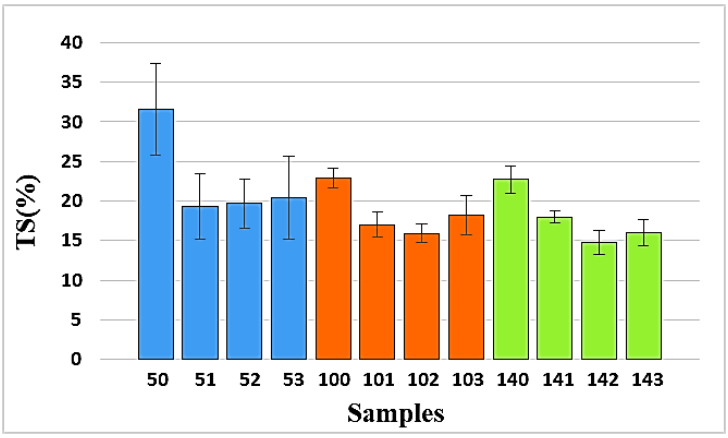

Figure 6. Effects of thickness and Nanomaterial on Thickness Swelling

2.3.3. Quasi-static properties

Quasi-static tests were carried out in a universal testing machine (Intron 4486) with a capacity of 300 (kN). The specimens used in the quasi-static tests are solid square panels with the side of 150 mm and a height of 5,10,14 mm. tests were performed with the strain rate of 5mm/min at room temperature under the quasi-static uniaxial conditions via a steel flat head indenter with 20mm diameter.

At first, the loading plane was tangent to the panels and then loading continued until the full perforation of the boards. By comparing strain rates obtained in numerical modeling and matching the results, it was assured that the test was completed in the quasi-static range. The force-displacement was recorded by the computer and used to extract other failure parameters. Each test repeated three times. Figure 7 shows the test procedure. To ensure that the board is not moving during the test, panels are equipped with 8 screws in the fixture.

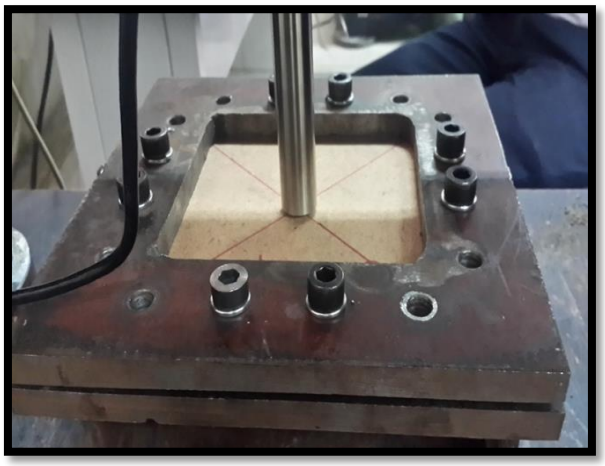

Figure 7. The quasi-static test procedure

Table 3. The overall mechanical and physical measurement results

No.	Density	IB	IB*	MOE	MOE*	MOR	MOR*	SAE	Absorbed Energy	Peak Load	TS	Water Absorption
	($kg.m^{-3}$)	(MPa)	(MPa)	(MPa)	(MPa)	(MPa)	(MPa)	(J/gr)	(J)	(N)	(%)	(%)
50	742	0.41	0.41	1679	1697.1	37.4	37.8	0.2163	6.49	667	31.6	95.7
51	824.4	0.48	0.43	2556.3	2325.6	46.7	42.5	0.254	7.62	731	19.3	61.5
52	754.2	0.64	0.64	2181	2168.9	39.5	39.3	0.247	7.41	800	19.7	64
53	723.6	1.06	1.1	1981.6	2053.9	36.7	38	0.202	6.06	654	20.4	73.7
100	803.6	0.31	0.29	2826.5	2638	29.2	27.3	0.2775	16.65	2172	22.9	84
101	838.2	0.66	0.59	3931.3	3517.7	44.2	39.5	0.3248	20.57	2485	17	49.7
102	891.8	0.74	0.62	3323.8	2795.3	39.2	33	0.2997	17.98	2757	15.9	58.5
103	828.4	0.79	0.72	2990.7	2707.7	31.2	28.2	0.315	18.9	2458	18.2	61.2
140	843.4	0.22	0.2	2930.1	2605.6	28.8	25.6	0.3448	28.96	3762	22.7	74.6
141	865.2	0.4	0.34	3328.8	2885.6	30.1	26.1	0.3458	29.05	4310	18	50
142	821.5	0.61	0.56	3429.3	3130.8	35.3	32.2	0.342	28.73	3883	14.8	48.8
143	853.3	0.65	0.57	3310.7	2909.9	35.5	31.2	0.3394	28.51	4226	16	57.2

As can be seen from the data table, there is a difference between the nominal density (750 $kg.m^{-3}$) and actual density(test values in Table 3) values. This difference is related to the press closing speed (Ee Ding 1998). For solving this problem, the method explained in Eq. (1) for adjusted properties (Xing et al. 2007), is applied to the mechanical properties in order to remove the effect of density. Starred values in Table 3 are modified values.

$$\text{Adjusted(MOR,MOE,IB)} = \frac{\text{test value} \times 750}{\text{specimen density}} \quad (1)$$

It should be noted that moisture exists in the process of making samples with fibers. It is realized that the rate of heat transfer after the addition of nano alumina to MDF, is higher. It has also improved its bonding strength (Anuj 2013). Therefore, during hot pressing, moisture transfer from the surfaces to the center, accumulation of vapor in the middle layers and formation of vapor pressure occurs. This vapor pressure after the removal of the load from the panels leads to spring back and cause heterogeneity in the vertical gradient of density and increases the density difference between the surface and the interlayers, hence the interlayers act as stress concentration points, and greatly affect the mechanical properties, especially the internal bonding. Therefore, as much as the thickness of the board and the volume of material used are more, the moisture content and the volume of water inside will be greater, and as a result, these events will be more intense. Thus, comparing the results of internal bonding and bending tests, it can be concluded that the addition of nano-alumina resulted in the enhancement of the adhesive so that, adding nanomaterials, improved IB, but compared with the results of bending tests, it can be said that in mechanical tests, the role of fiber quality, the manufacturing conditions and thickness are more powerful than the nanoscale materials.

3. Simulation of quasi-static test

The scope of this part of the research is to focus on the macrostructure modeling of wooden composites. The disadvantage in describing the mechanical properties of wood on the macro scale is the trouble predicting the non-linear behavior (Nilsen 2015). The mechanical properties of wood in the elastic range are relatively easily described. Difficulties arise when describing nonlinear mechanical properties. Wood is characterized as brittle in tension, shear and ductile in compression.

All the following simulated in ABAQUS 6.17 and ran with the Dynamic, Explicit method. For modeling the specimen in the software, MDF panels are simulated three dimensional, deformable under quasi-static load while the indenture is considered solid. The calculated results have been compared to earlier experimental results from the literature. For interaction between the surfaces of the indenture and the board during contact, a surface-to-surface option is used. The friction between the collision surfaces was simulated with a friction coefficient of $\mu = 0.3$ (TS. 2015). The type of contact is considered hard contact. The kinetic energy stayed under 10% of the internal energy. It reveals that the value of the kinetic energy is a tiny part of the value of the total strain energy, which means that all the external work nearly equals to the total strain energy of the system. Such a quasi-static compression simulation is qualified. In the material definition, the material parameters have to be defined. Hence, it is necessary to use the **User material** key words to define the required parameters (Mirianon et al. 2008).

For modeling the failure, the Hashin failure criterion was used. Because the two-dimensional Hashin failure criterion is not able to predict the behavior of composite failure, by using the VUMAT code, the three-dimensional Hashin by coupling FORTRAN with ABAQUS has been used. According to the test conditions, the boundary conditions of the board were considered as clamped. For meshing the 5 mm board, 23512 nodes and 17282 elements were assumed to be hexagonal 3D elements (C3D8R). The dimension of each mesh is 0.002 which is approximately 2 mm in 2 mm and 2 mm in thickness. Mesh convergence has been investigated in sizes of 5, 3, 2, and 1 mm. solutions in 2 and 1 mm mode were both converged. Because of the higher problem-solving time in 1 mm mesh mode and good accuracy of the solutions in 2mm, mesh size of 0.002 was used. Meshes are Explicit and 3D Stress. Element deletion was used to remove elements after full energy absorption. For the rigid indenture with a diameter of 20 mm, length of 120 mm and a weight of 331.29 g, the properties of ordinary steel were assigned. Since the experimental tests were performed with a 5 mm/min strain rate in a time period of 60 seconds, these values attributed to the indenter as well.

Among the 17 parameters needed to define the Hashin 3-D failure criterion, elastic properties and tensile strengths were obtained using standard tests. Compressive strength and compression stress were also required. Commonly, stiffness and strength values can be obtained only with difficulty because of the two main issues which are the inherent large distribution of wood's mechanical properties and difficulties connected with testing and measuring (Moses and Prion 2004). Compressive stress, due to the lack of standard tests for MDF boards in compression mode, are extracted from existing researches with similar properties and are presented in Table 4. Figure 8 illustrates the meshed board and the indenture.

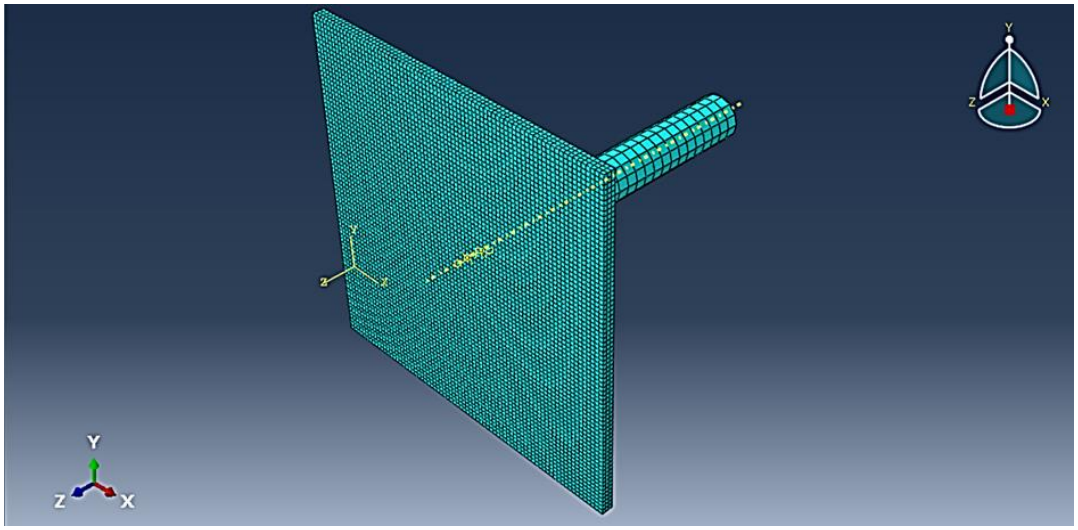

Figure 8. Modelling the 5mm meshed panel and the meshed indenture

Table 4. Mechanical properties of the composite used in the simulation (TS. 2015)

Property	Symbol	Value
Principal Poisson's ratio	υ12	0.2
Shear modulus (GPa)	G12	5
Longitudinal tensile strength (MPa)	S1t	150
Longitudinal compressive strength (MPa)	S1c	150
Transverse Tensile strength (MPa)	S2t	50
Transverse compressive strength (MPa)	S2c	50
In-plain Shear strength (MPa)	S12	50
Tensile failure stress (MPa)	NFLS	150
Shear failure stress (MPa)	SFLS	50

4. Degradation mechanisms and energy absorptions

In all of the quasi-static samples tested, failure was occurred by layering out. Figure 9 shows the quasi-static degradation of boards in different thicknesses. As can be seen from Figure 9, by increasing the thickness of the panels, the extent of destruction and layering increased. In Figure 9a, two petals are created while in Figure 9b, 3 petals can be seen. Figure 10 shows the load-deformation diagram of the 5 mm panel after the test. From Figure 10, it is realized that the linear part is the elastic region and is related to the bending of the panel. At the end of the elastic region, which deflects with layering out and formation of petalling, the maximum force at this point was achieved. Note that, broken layers remained unified in all tests and did not split into fragments, which can be reasonably attributed to the integrity of the structures used. After the peak load, the force decreases steadily, indicating the continuous destruction and the rear surface are broken as the indent continues and interlayer cracks grow. As stated by other researchers, the continuous destruction of composite boards is accompanied by the accumulation of crushed fibers and resin in internal cracked layers (Hoo Fatt and Lin 2004). This continuous behavior was stable until more than half of the thickness of the boards and accompanied by increasing force in the force-

displacement curve. This was due to the accumulation of layers of fibers bent in the space of the board. Thereupon, the composite saturation point is attained. In the tested specimens, the broken layers are visible, which in particular, as it is shown in Figure 9, are clearly visible on the outer surface, which bends considerably over more than the other layers.

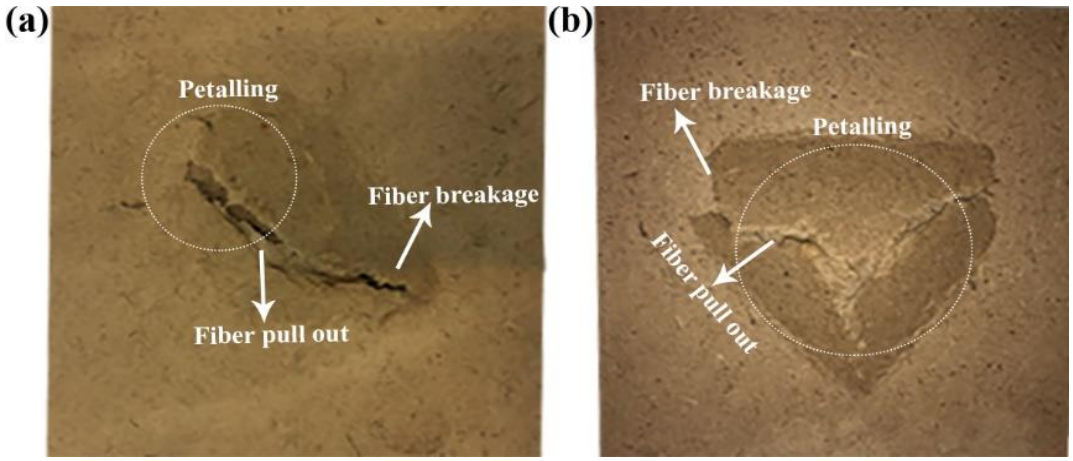

Figure 9. Failure of composite boards under quasi-static load, a) 10mm panel backplate, b) 14mm panel backplate

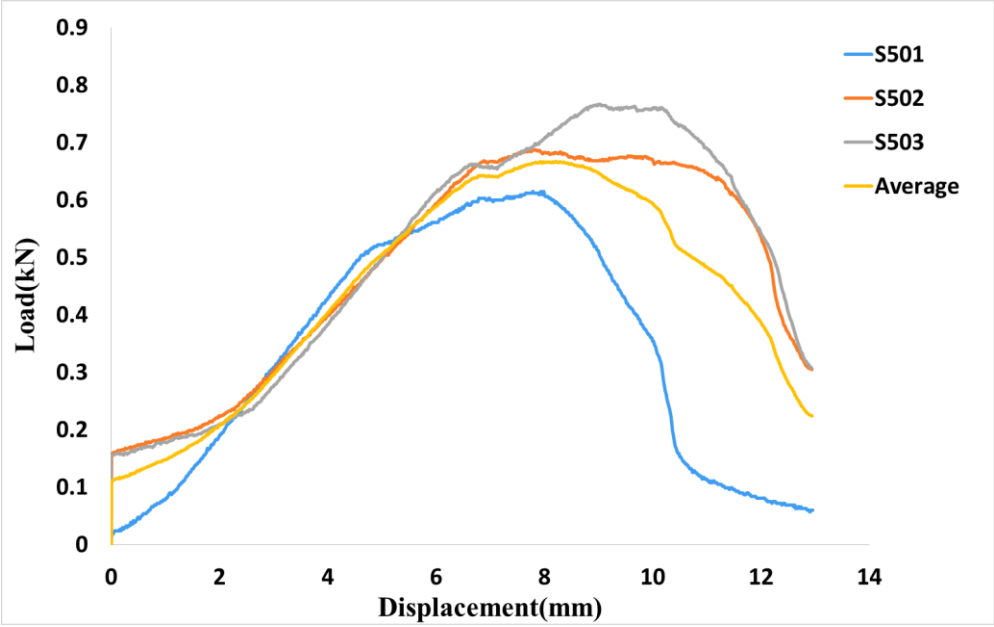

Figure 10. Load-deformation diagram under quasi-static load for a 5mm panel

To properly analyze the behavior of composites and the impact of different parameters in damage, the examination of the mechanisms involved in destruction and energy absorption is necessary. From Figure 11, it is clear that different mechanisms play a role in this problem. These mechanisms

include matrix compression and tension failure, interlayer cracks, the formation of intra-layer cracks and bending of layers. Panel deformation takes place on two scales:
1) Local: indentation of the indenture through-thickness.
2) Global: due to shear, bending or membrane deformation of the plate.
The clamping composite plate undergoes localized indentation, shear, bending, or membrane elongation before perforation. One or more of these deformation modalities can be dominant due to the aspect ratio (a /h) of the structure, which is defined in Figure 11.
In the present study, in order to understand the failure modifications, three aspect ratios (30, 15, and 10.7) were studied. The following results were obtained:

1- The board with a/h= 30 had large deformations and entered the membrane phase before tensile necking.
2- The boards with a/h= 15 and a/h=10.7 behaved relatively similarly. In 10 and 14 mm boards, at first, the front surface destroyed and then by indenture precession the back surface failed. This behavior was due to the combination of local indentation, general deformation, and shear in boards. While in 5 mm boards, at first, the back surface began to crack and demolished, and then with increasing inclination, the upper plate was destroyed. The bending behavior was dominant and general energy absorption occurred.
3- The greatest amount of energy absorption in layering and deformation has occurred.

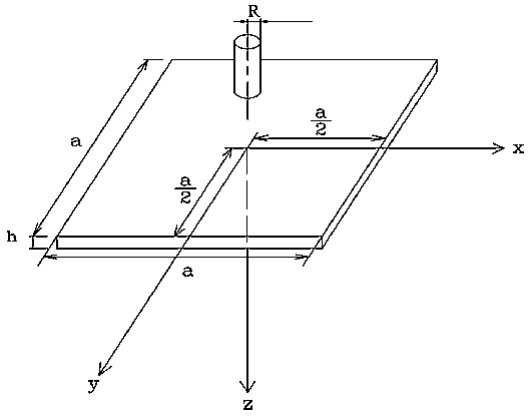

Figure 11. The geometry of specimens and the definition of aspect ratio (a/h) (Hoo Fatt and Lin 2004)

The load-deformation curves from the average of three iterations of the experimental tests are plotted in Figure 12.

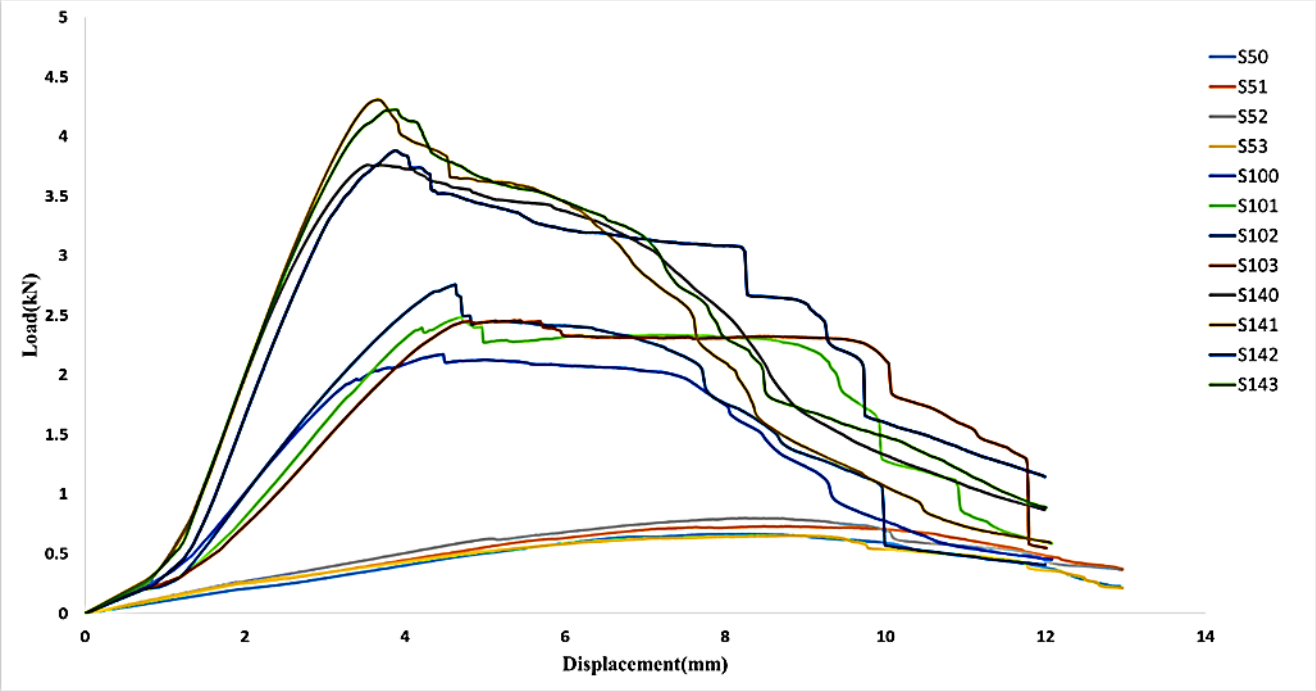

Figure 12. Load-deformation curves of the experimental results

As may be seen from Figure 12, the thickness of the panels is a very important and prominent factor in the behavior of these structures. Three levels of energy for thickness 5, 10 and 14 mm are clearly visible. By increasing the thickness of the panels, growth in the linear region and maximum force is observed. However, increasing the amount of energy absorption shows that the volume of damage has also enlarged. Increasing the thickness of the boards intensifies the amount of energy necessary to collect the layers inside the boards and form more rigid layers, therefore reduce the bending radius in the matrix fracture area. Nevertheless, a linear trend in maximum force and energy absorption variations is not observed as a function of the alumina percentage, which is attributed to the agglomeration of nanoparticles in higher alumina amounts. To further examine the distribution of nanoparticles, FESEM images taken from 0, 1, 2 and 3% Nano-alumina samples. As can be seen from Figure.13b Nanoparticles are aggregated in samples containing 3% nanoparticles and created a heterogeneous structure.

The failure parameters including maximum force, energy absorption and specific energy absorption are shown in Table 3. In 5, 10 and 14 mm boards, the highest peak loads belong to samples containing 2%, 2% and 1% alumina, respectively. In all thicknesses, the highest energy absorption was found in samples with 1% nanoparticles. By adding 1% Nano alumina to 5, 10 and 14 mm boards, the energy absorption was increased 17%, 24%, and 0.3% respectively.

Therefore, in general, the addition of nanomaterial has improved peak load, energy absorption and specific energy absorption of the boards.

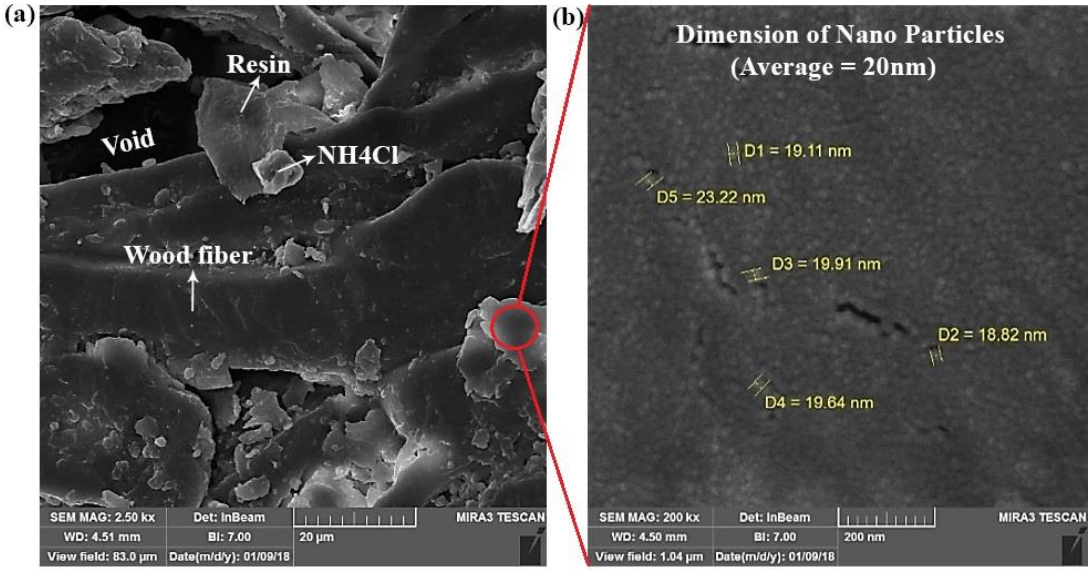

Figure 13a. FESEM image of MDF particles (a) S100 magnified 20µm (b) S100 magnified 200nm

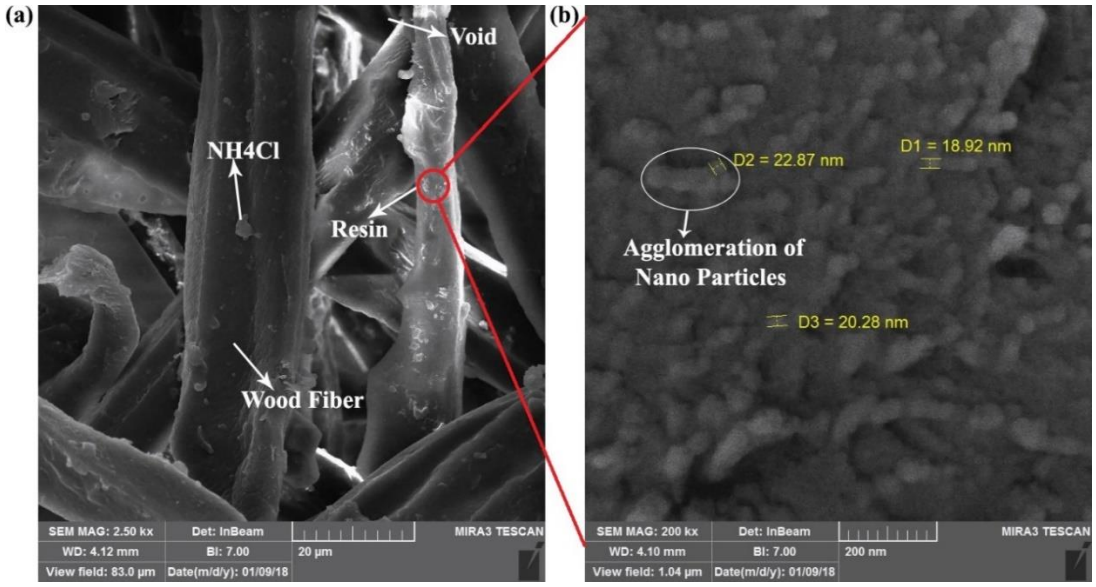

Figure 13b. FESEM image of MDF particles (a) S103 magnified 20µm (b) S103 magnified 200nm

Figure 14 illustrates the comparison between the numerical and experimental results in a load-deformation diagram for a 5mm witness panel. By plotting experimental test results with the load-deformation curve from ABAQUS at the same chart, it was realized that the obtained elastic-plastic behavior is appropriate for this kind of material. The comparison shows good agreements.

The numerical simulation of quasi-static indentation for a 5mm witness board is shown in Figure 15. The layering, bending of the layers in the outer surface, and the petalling have been well recognized in the modeling. For more modeling accuracy and verifiability, 10 and 14 mm boards were also modeled in the same way and the parameters are presented in Table 5 and compared with the experimental results. As can be seen, the modeling error in all cases is less than 10% and the 5 mm board is less than 5%. This indicates that the simulation strategy has been efficiently

applied and the structural model used has the ability to consider all damage parameters and energy absorption.

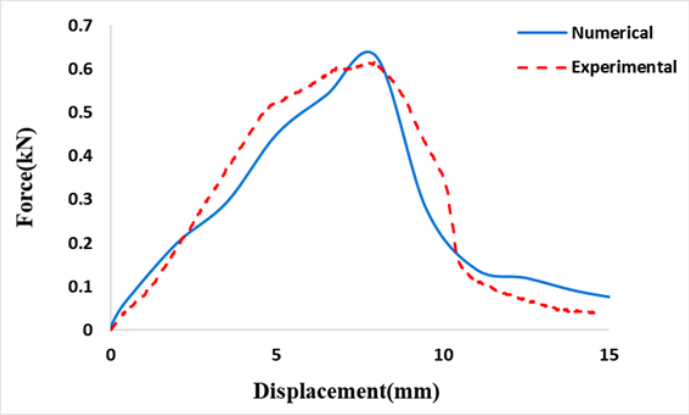

Figure 14. Comparing numerical and experimental results for S50

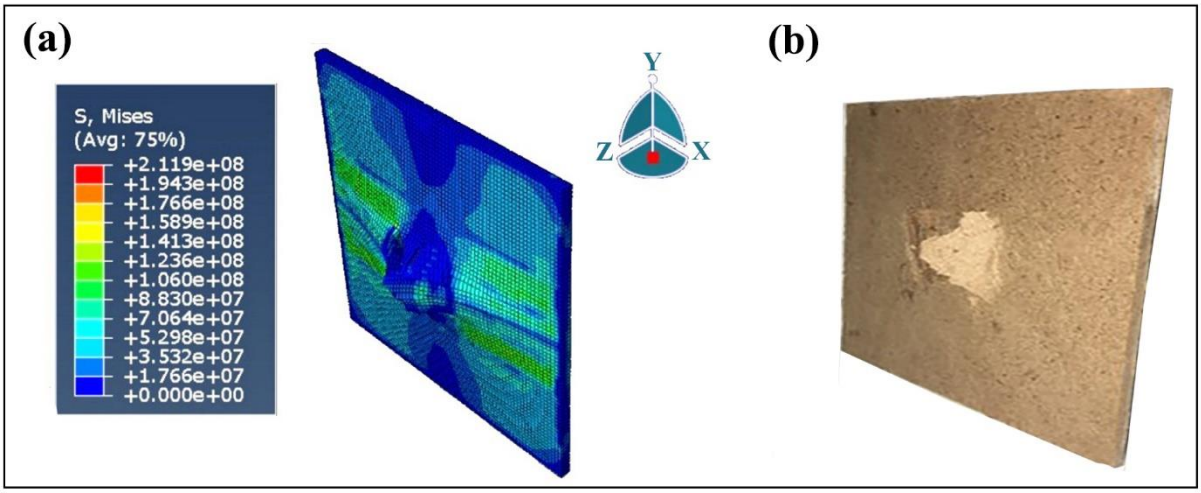

Figure 15. Failure of S50 in the quasi-static indentation, a) Numerical simulation, b) Experimental test result

Table 5. Results of numerical simulation for quasi-static indentation

Specimen	Peak Load(N)	Error (%)	Absorbed Energy(J)	Error (%)	SAE (J/g)	Error (%)
50	694	4	6.74	3.9	0.225	4.6
100	2363	8.8	16.75	0.6	0.292	5.3
140	4015	6.7	29.45	1.7	0.351	2.9

5. Results and discussion

As can be seen from Figure 3a, the highest modulus of elasticity in bending test in 5,10 and 14mm panels achieved in 1,1 and 2% wt. Nano percentage, respectively. Increasing the thickness of the boards increased their stiffness. In 5mm panels, an increase of 1, 2 and 3 percent of Nano alumina resulted in an increase of 37, 27 and 21 percent in the MOE, respectively. In 10mm panels, an increase of 1, 2 and 3 percent of Nano alumina resulted in an increase of 33, 6 and 3 percent in the MOE, respectively and in 14mm panels, an increase of 1, 2 and 3 percent of Nanoparticles caused to 11, 20 and 12 percent increase in the MOE, respectively. In general, Adding nanoparticles to the boards has a positive effect on increasing the MOE and their stiffness. This increment in MOE might be attributed to the high stiffness caused by the decrease in mobility of the fibers that were placed between the Nano Al_2O_3 particles (Deka and Maji 2011b). A similar result was observed for 2% Nano clays in Ref. (Chavooshi et al. 2014). Their FE-SEM and XRD observations showed that 2% by weight of Nano clay had overall better performance than other percentages because of the better formation of an intercalated nanostructure (Chavooshi et al. 2014).

Figure 3b shows that the addition of Nano Al_2O_3 particles resulted in an enhancement in MOR. It can be seen that by increasing the thickness of the MDF panels from 5mm to 14mm, the modulus of rupture decreases. The similar results were reported in (Alamri and Low 2013). The greatest increase in MOR was achieved when 1,1,2% wt. Nano Al_2O_3 was added to the 5, 10 and 14mm samples. The addition of 1, 2 and 3 wt. % Nano Al_2O_3 in 5mm samples led to 12, 4 and 0.5 % increase in MOR, respectively. In 10mm boards, the addition of 1, 2 and 3 wt. % Nano Al_2O_3 resulted in 47, 21 and 3 % increase in MOR, respectively. In 14mm samples, the addition of 1, 2 and 3 wt. % Nano Al_2O_3 caused to 2, 26 and 22 % increase in MOR, respectively.

It may be seen from Figures 4, by increasing the thickness, IB has been steadily declining and by addition of Nano percentages, IB has increased progressively. The results show a good interaction between the fibers matrix and Al_2O_3 particles.

To analyze the results more accurately, statistical analysis was performed on the physical and mechanical test results. Given that all the coefficient of variation calculated is less than 30, therefore the data are acceptable and can be cited to compare.

Regarding Figure 5, in 5mm samples, with the increase in the nanomaterials percentage, the amount of water absorption decreases, so that the increase of 1, 2 and 3% of nano alumina resulted in 36, 33 and 23% decrease in WA, respectively. In 10mm boards, adding 1, 2 and 3% nano alumina resulted in 41, 30 and 27% decrease in WA, respectively. In 14 mm panels, by increasing the percentage of nanomaterials, the amount of water absorption has decreased 33, 35 and 23% respectively. In all thicknesses, the highest water absorption was obtained in witness samples.

From Figure 6, in 5mm samples, with the increase in the nanomaterials percentage, the amount of TS decreases, so that the increase of 1, 2 and 3% of nano alumina resulted in 39, 38 and 35% decrease in TS, respectively. In 10mm boards, adding 1, 2 and 3% wt. Al_2O_3 resulted in 26, 25 and 21% decrease in WA, respectively. In 14 mm panels, by increasing the percentage of nanomaterials, the amount of water absorption has decreased 21, 35 and 30% respectively. In all thicknesses, the highest TS belonged to the witness samples.

5.1. Relationship between water absorption and thickness swelling

Water absorption depends directly on the density and porosity of the boards where water can be trapped among the fibers. The density will have a significant effect on water absorption and thickness swelling, which will cause errors in the results. Since the fibers are not homogeneous, this structure can lead to a poor resin distribution and also inadequate bonding, which can have a negative effect, especially on physical properties. Figure 16 shows the relation between thickness swelling and water absorption. The tolerance in density affects physical properties and makes it difficult to find the appropriate relationship between water absorption and thickness swelling, However, the coefficient of correlation R^2, which is between zero and one, confirms the existence of a linear relationship between WA and TS in this case.

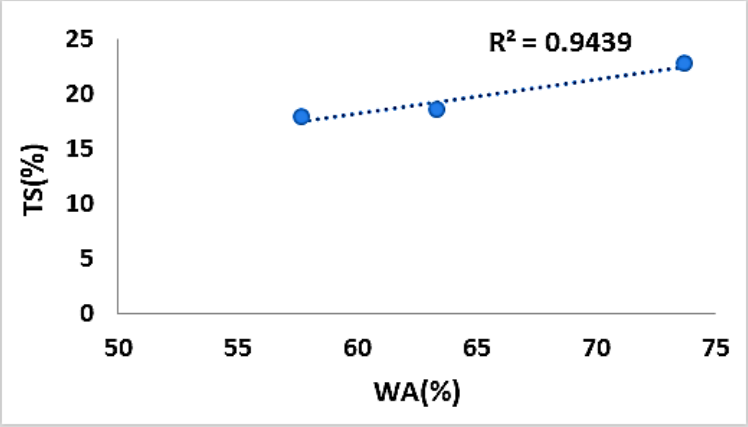

Figure 16. Relationship between water absorption and thickness swelling for 5, 10 and 14mm panels

6. Conclusions

In this research, the effect of adding Nano Al_2O_3 (0, 1, 2 and 3 weight percentages) to MDF panels (5, 10 and 14 mm thicknesses) was investigated and based on the experimental results the following conclusion have been made:

- By increasing the thickness, IB has been steadily declined and by the addition of Nano percentages, IB has been progressively increased.
- The greatest increase in MOE was achieved when 1, 1 and 2% wt. Nano Al_2O_3 was added to the 5, 10 and 14 mm samples, respectively. It was observed that in 5, 10 and 14 mm boards, MOE increased 37, 33 and 20% respectively.
- By increasing the thickness of the MDF panels from 5mm to 14mm, MOR decreases.
- The greatest increase in MOR was achieved when 1,1,2% wt. Nano Al_2O_3 was added to the 5, 10 and 14mm samples. It was observed that in 5, 10 and 14 mm boards, MOR increased 12, 47 and 26% respectively.
- The results showed that the addition of Nano Al_2O_3 to the MDF composites reduces WA and TS.
- From the experimental results, TS has a linear relation with WA.
- By increasing the thickness of the boards, both WA and TS decreased.
- Energy absorption and a peak load of the composites containing Nanoparticles were higher compared to witness samples.

- Addition of Al_2O_3 Nano-particles up to 1 weight percentage in 5, 10 and 14 mm panels amplified energy absorption as 17, 24 and 0.3%, respectively.
- Increasing the thickness of the panels from 5 to 14 mm improved peak load and energy absorption up to 82% and 78%, respectively.
- The greatest increase in peak load and energy absorption was observed in samples with 2 and 1 weight percentage Nano Al_2O_3, respectively.
- There was a good agreement between the numerical and experimental results.
- So as to realize the failure mechanisms, three aspect ratios (30, 15, and 10.7) were studied. The following results were obtained:
    - The board with a/h= 30 had large deformations and entered the membrane phase before tensile necking.
    - The boards with a/h= 10.7,15 behaved similarly. Local indentation, general deformation and shear occurred, while in 5 mm boards, the bending behavior was dominant.
    - The greatest amount of energy absorption in layering and deformation has occurred.

Generally, the addition of Nanoparticles had a positive impact on increasing MOR and MOE of panels. The agglomeration of nanoparticles in 2, 3% Nano-alumina has made an optimum limit for the addition of nano-alumina to the boards, while 1% nano-alumina dispersed and intercalated better through the panels.

Due to the high strength of wooden products with respect to their weight and low cost, MDF is considered an excellent material for industries such as building and construction. Hence, by reinforcing MDFs with other components such as Nanoceramics, durability, and strength of them can be increased. Nano Al_2O_3, are environment-friendly and can be properly seen as an alternative for reinforcing wooden composites.

Abbreviations

APS	Average Particle Size
ASTM	American Society for Testing and Materials
CAI	Compression After Impact
CV	Coefficient of Variation
EDS	Energy Dispersive X-Ray Analysis
EN	European Norm
FESEM	Field Emission Scanning Electron Microscopy
IB	Internal Bonding
MDF	Medium Density Fibreboards
MOE	Modulus of Elasticity
MOR	Modulus of Rupture
SAE	Specimen Mass Absorbed Energy
TS	Thickness Swelling
UF	Urea Formaldehyde
WA	Water Absorption

Disclosure statement

No potential conflict of interest was reported by the authors.

References

Abrate, S. 1991. Impact on Laminated Composite Materials. *Applied Mechanics Reviews,* 44(4), 155-190.

Abrate, S., 2011. *Impact Engineering of Composite Structures.* Springer Vienna.

Aisyah, H. A.*, et al.* 2013. Properties of medium density fibreboard (MDF) from kenaf (Hibiscus cannabinus L.) core as function of refining conditions. *Composites Part B: Engineering,* 44(1), 592-596.

Alamri, H. and Low, I. M. 2013. Effect of water absorption on the mechanical properties of nanoclay filled recycled cellulose fibre reinforced epoxy hybrid nanocomposites. *Composites Part A: Applied Science and Manufacturing,* 44, 23-31.

Anuj, K. A., Gupta ; K. V. , Sharma ; M. , Nasir; 2013. Use of aluminum oxide nanoparticles in wood composites to enhance the heat transfer during hot-pressing. *Eur. J. Wood Prod.,* 71(2), 193–198.

Arabi, M.*, et al.* 2011. Interaction analysis between slenderness ratio and resin content on mechanical properties of particleboard. *Journal of Forestry Research,* 22(3), 461.

Assaedi, H., Shaikh, F. U. A. and Low, I. M. 2016. Characterizations of flax fabric reinforced nanoclay-geopolymer composites. *Composites Part B: Engineering,* 95(Supplement C), 412-422.

Ates, S.*, et al.* 2017. Effects of heat treatment on some properties of MDF (medium-density fiberboard). *Wood Material Science & Engineering,* 12(3), 158-164.

Balıkoğlu, F.*, et al.* 2018. Compression after low velocity impact tests of marine sandwich composites: Effect of intermediate wooden layers. *Composite Structures,* 183(Supplement C), 636-642.

Benmansour, N.*, et al.* 2014. Thermal and mechanical performance of natural mortar reinforced with date palm fibers for use as insulating materials in building. *Energy and Buildings,* 81, 98-104.

BS-EN-310, 1993. Wood-based panels. Determination of modulus of elasticity in bending and of bending strength. British Standards Institution, London.

BS-EN-317, 1993. Particleboards and fibreboards. Determination of swelling in thickness after immersion in water. British Standards Institution, London.

BS-EN-319, 1993. Particleboards and fibreboards. Determination of tensile strength perpendicular to the plane of the board. British Standards Institution, London.

BS-EN-322, 1993. Wood-based panels. Determination of moisture content. British Standards Institution, London.

BS-EN-323, 1993. Wood-based panels. Determination of density. British Standards Institution, London.

Cantwell, W. J. and Morton, J. 1991. The impact resistance of composite materials — a review. *Composites,* 22(5), 347-362.

Chavooshi, A.*, et al.* 2014. MDF dust/PP composites reinforced with nanoclay: Morphology, long-term physical properties and withdrawal strength of fasteners in dry and saturated conditions. *Construction and Building Materials,* 52, 324-330.

Deka, B. K. and Maji, T. K. 2011a. Effect of TiO2 and nanoclay on the properties of wood polymer nanocomposite. *Composites Part A: Applied Science and Manufacturing,* 42(12), 2117-2125.

Deka, B. K. and Maji, T. K. 2011b. Study on the properties of nanocomposite based on high density polyethylene, polypropylene, polyvinyl chloride and wood. *Composites Part A: Applied Science and Manufacturing,* 42(6), 686-693.

Ee Ding, W. M., Zhang; Qian, Wang; Shuichi, Kawai; 1998. Effects of mat moisture content and press closing speed on the formation of density profile and properties of particleboard. *Journal of Wood Science,* 44(4), 287–295.

Esmailpour, A*., et al.* 2019. Nano-wollastonite to improve fire retardancy in medium-density fiberboard (MDF) made from wood fibers and camel-thorn. *Wood Material Science & Engineering*, 1-5.

Fortin-Smith, J*., et al.* 2016. Characterization of Maple and Ash Material Properties as a Function of Wood Density for Bat/Ball Impact Modeling in LS-DYNA. *Procedia Engineering,* 147(Supplement C), 413-418.

Glé, P., Gourdon, E. and Arnaud, L. 2011. Acoustical properties of materials made of vegetable particles with several scales of porosity. *Applied Acoustics,* 72(5), 249-259.

Haseli, M., Layeghi, M. and Zarea Hosseinabadi, H. 2018. Characterization of blockboard and battenboard sandwich panels from date palm waste trunks. *Measurement,* 124, 329-337.

Hazrati-Behnagh, M*., et al.* 2016. Mechanical and insulating performances of ultralight thick particleboard from sugarcane residues and woods planer shaving. *European Journal of Wood and Wood Products,* 74(2), 161-168.

Hoo Fatt, M. S. and Lin, C. 2004. Perforation of clamped, woven E-glass/polyester panels. *Composites Part B: Engineering,* 35(5), 359-378.

Jonoobi, M*., et al.* 2017. Effect of surface modification of fibers on the medium density fiberboard properties. *European Journal of Wood and Wood Products*.

Jover, N., Shafiq, B. and Vaidya, U. 2014. Ballistic impact analysis of balsa core sandwich composites. *Composites Part B: Engineering,* 67(Supplement C), 160-169.

Koli, D. K., Agnihotri, G. and Purohit, R. 2014. A Review on Properties, Behaviour and Processing Methods for Al- Nano Al2O3 Composites. *Procedia Materials Science,* 6, 567-589.

Liu, T*., et al.* 2017. Energy absorption characteristics of sandwich structures with composite sheets and bio coconut core. *Composites Part B: Engineering,* 114(Supplement C), 328-338.

Mantanis, G. I*., et al.* 2018. Adhesive systems used in the European particleboard, MDF and OSB industries. *Wood Material Science & Engineering,* 13(2), 104-116.

Mantanis, G. I*., et al.* 2019. Technological properties and fire performance of medium density fibreboard (MDF) treated with selected polyphosphate-based fire retardants. *Wood Material Science & Engineering*, 1-9.

Mirianon, F*., et al.*, 2008. *A Method to Model Wood by Using ABAQUS Finite Element Software: Part 2. Application to Dowel Type Connections.* VTT Technical Research Centre of Finland.

Moses, D. M. and Prion, H. G. L. 2004. Stress and failure analysis of wood composites: a new model. *Composites Part B: Engineering,* 35(3), 251-261.

Nilsen, T. S., 2015. *Numerical modelling of Wood Microstructure.* (Master degree). Norwegian University of Science and Technology.

Olmedo, I*., et al.* 2016. Discrete element model of the dynamic response of fresh wood stems to impact. *Engineering Structures,* 120(Supplement C), 13-22.

Rathke, J*., et al.* 2012. Fracture energy vs. internal bond strength – mechanical characterization of wood-based panels. *Wood Material Science & Engineering,* 7(4), 176-185.

TS., N. 2015. Numerical modelling of Wood Microstructure: Norwegian University of Science and Technology.

Vaidya, U. K., 2011. Impact Response of Laminated and Sandwich Composites. *In:* Abrate, S. ed. *Impact Engineering of Composite Structures.* Vienna: Springer Vienna, 97-191.

Xing, C., Deng, J. and Zhang, S. Y. 2007. Effect of thermo-mechanical refining on properties of MDF made from black spruce bark. *Wood Science and Technology,* 41(4), 329-338.

Yoshihara, H. and Yoshinobu, M. 2015. Measurement of the in-plane shear modulus of medium-density fibreboard by torsional and flexural vibration tests. *Measurement,* 60, 33-38.